

## Supporting Information

### **Bis(aminothiolato)nickel Nanosheet as a Redox Switch for Conductivity and an Electrocatalyst for the Hydrogen Evolution Reaction**

Xinsen Sun,<sup>a</sup> Kuo-Hui Wu,<sup>a</sup> Ryota Sakamoto,<sup>a</sup> Tetsuro Kusamoto,<sup>a</sup> Hiroaki Maeda,<sup>a</sup>  
Xiaojuan Ni,<sup>b</sup> Wei Jiang,<sup>b</sup> Feng Liu,<sup>b</sup> Sono Sasaki,<sup>c,d</sup> Hiroyasu Masunaga<sup>e</sup> and Hiroshi  
Nishihara<sup>a\*</sup>

<sup>a</sup>Department of Chemistry, School of Science, The University of Tokyo, 7-3-1, Hongo, Bunkyo-ku, Tokyo, 113-0033 Japan

<sup>b</sup>Department of Materials Science and Engineering, University of Utah, Salt Lake City, UT 84112, USA

<sup>c</sup>Faculty of Fiber Science and Engineering, Kyoto Institute of Technology, Matsugasaki Hashikami-cho 1, Sakyo-ku, Kyoto 606-8585, Japan

<sup>d</sup>RIKEN SPring-8 Center, Kouto 1-1-1, Sayo-cho, Sayo-gun, Hyogo 679-5148, Japan

<sup>e</sup>Japan Synchrotron Radiation Research Institute (JASRI)/SPring-8, 1-1-1 Kouto, Sayo-cho, Sayo-gun, Hyogo 679-5198, Japan

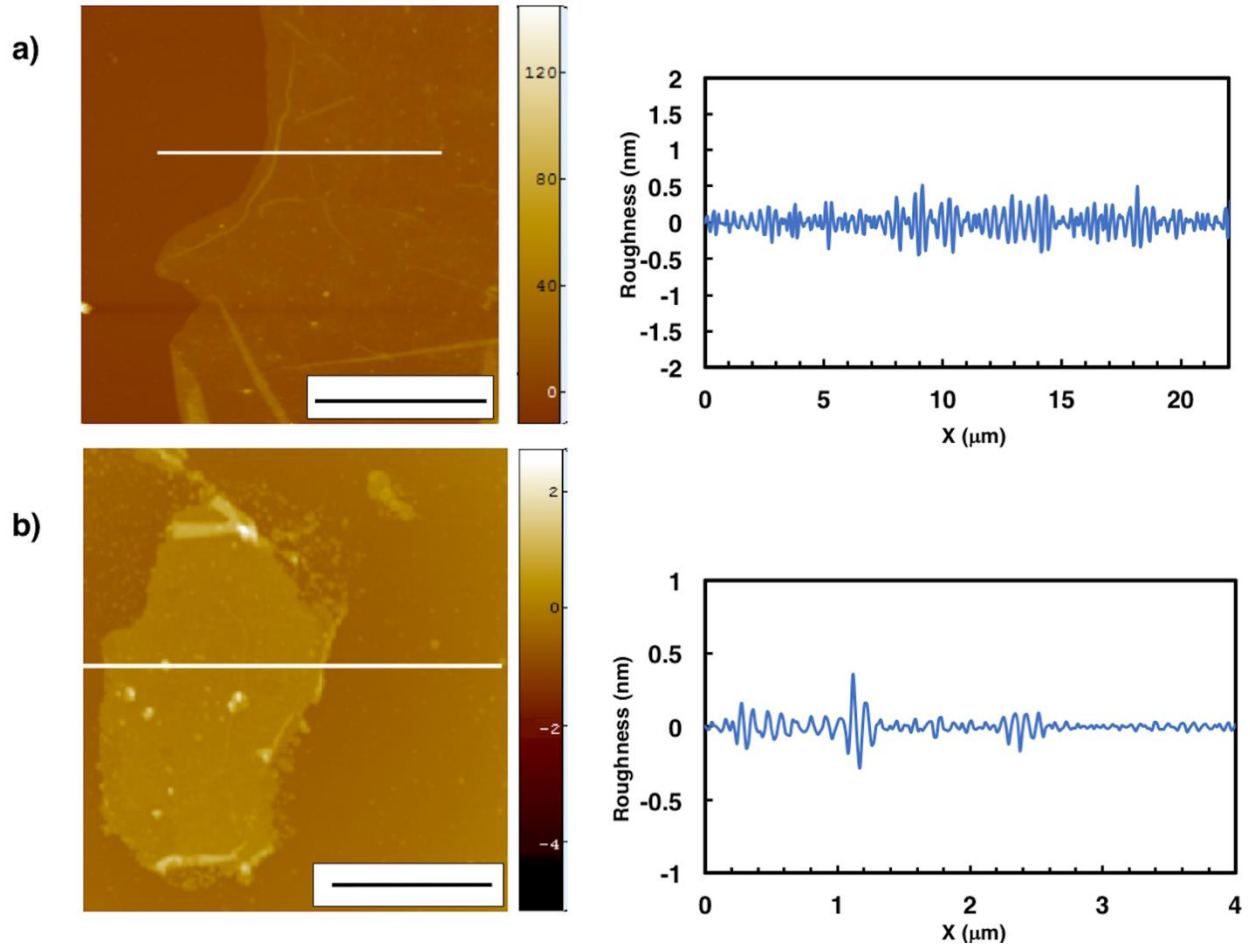


Fig. S1. **a)** AFM image on HMDS/Si(111) with height distribution indication and its roughness analysis along the cross-section white line of the multi-layer. Scale bars represent 10 μm. **b)** AFM image on HMDS/Si(111) with height distribution indication and its roughness analysis along the cross-section white line of the single-layer. Scale bars represent 2 μm.

IR spectra of NiIT, NiAT and ligand L (Fig. S2)

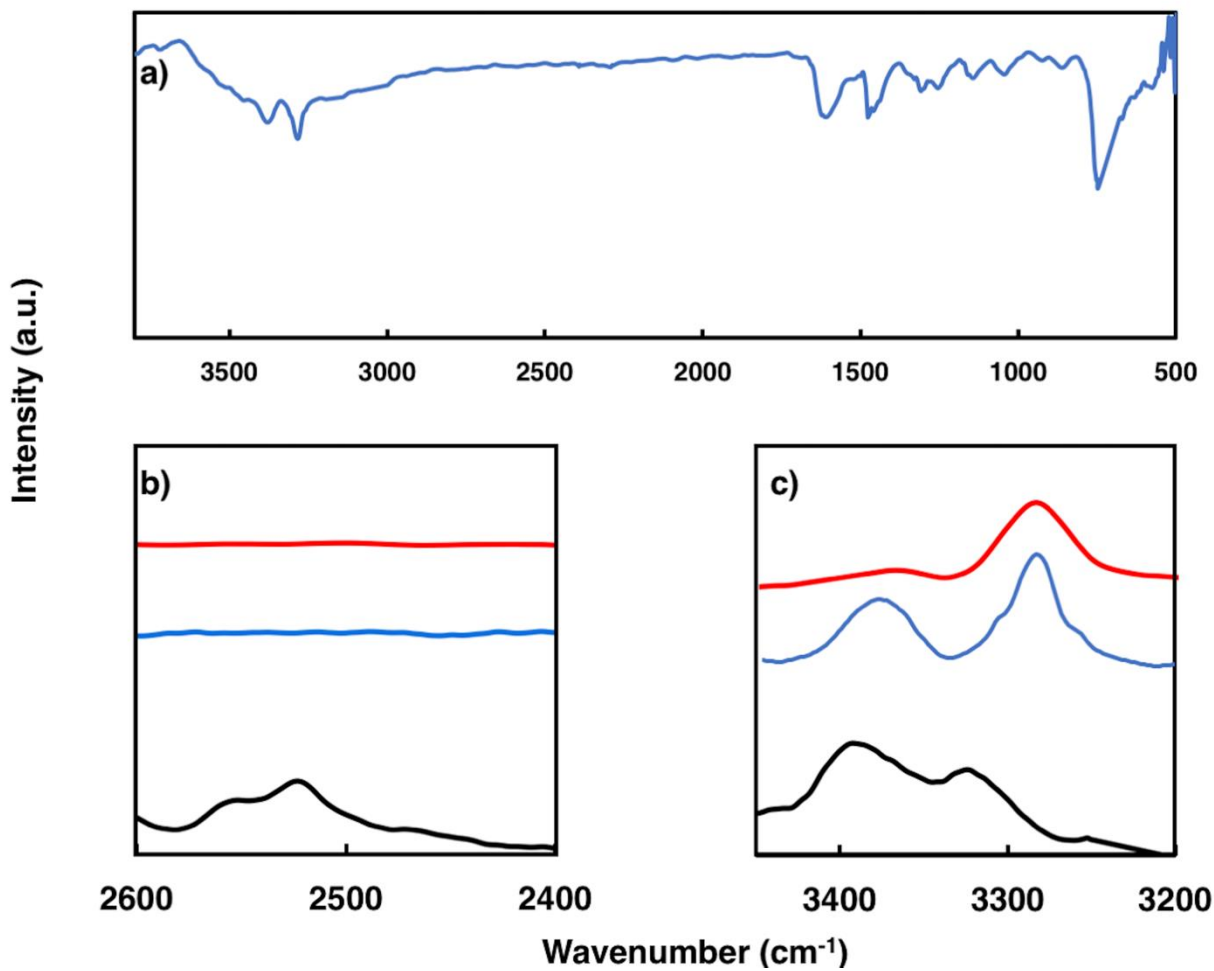


Fig. S2. **a)** Full IR spectra using ATR method of NiAT. Comprising of NiIT (red), NiAT (blue) and L (black). **b)** Focusing S-H stretching. **c)** Focusing on N-H stretching.

XPS of ligand **L** (Fig. S3)

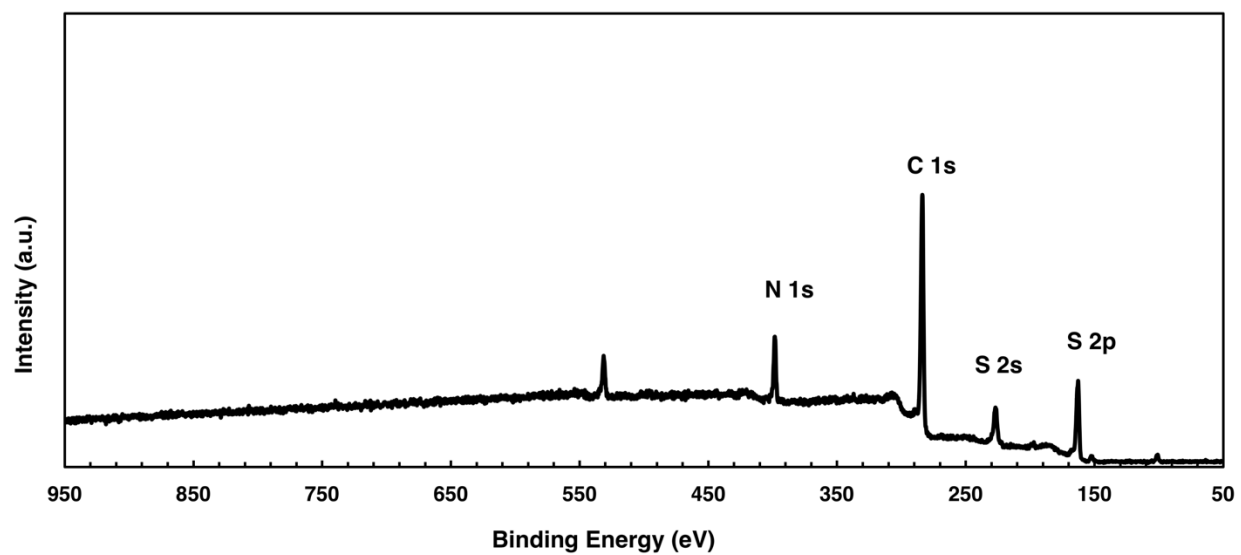


Fig. S3. Wide-scan XPS of ligand **L**.

XPS of mononuclear NiAT-M (Fig. S4)

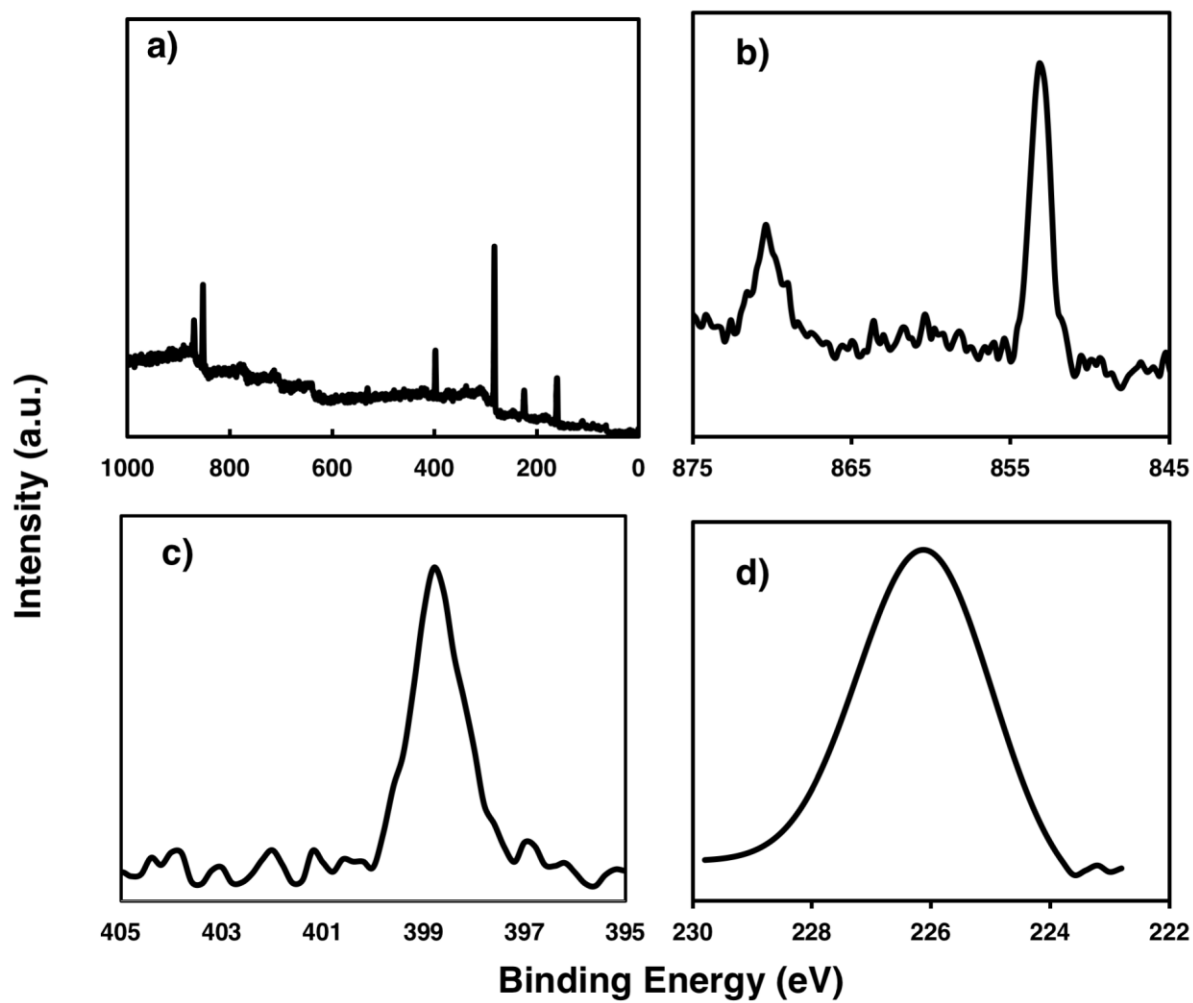


Fig. S4. **a)** Wide-scan XPS of NiAT-M. Narrow-scan XPS focusing on **b)** the Ni 2p region, **c)** the N 1s region, **d)** the S 2s region

XPS of mononuclear **NiIT-M** (Fig. S5) and **NiIT** (Fig. S6)

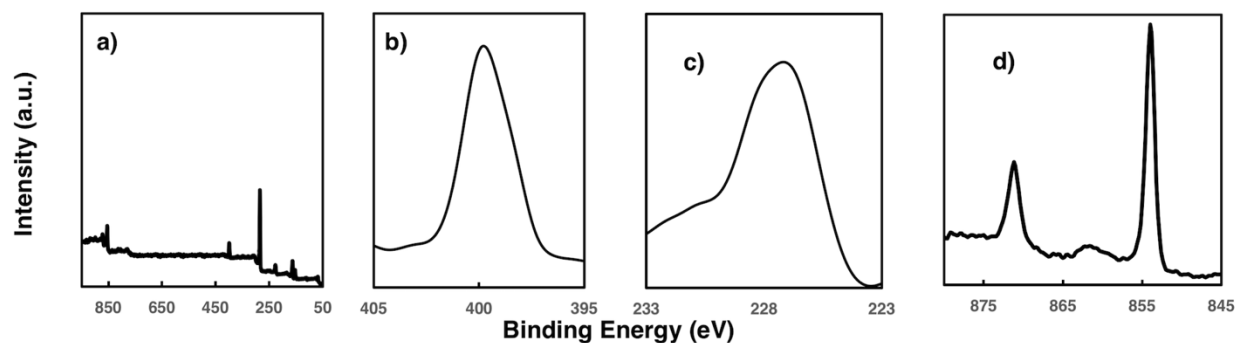


Figure S4. **a)** Wide-scan XPS of **NiIT-M**. Narrow-scan XPS focusing on **b)** the N 1s region, **c)** the S 2s region. **d)** the Ni 2p region,

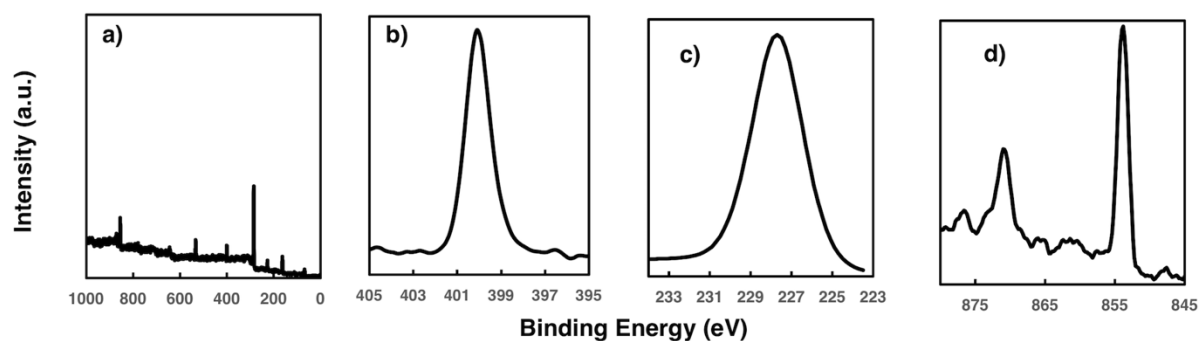


Fig. S5. **a)** Wide-scan XPS of **NiIT**. Narrow-scan XPS focusing on **b)** the N 1s region, **c)** the S 2s region. **d)** the Ni 2p region.

Table S1. XPS of N 1s and S 2s peak regions combined table

	<b>N 1s/eV</b>	<b>S 2s/eV</b>
L	400.2	227.8
NiIT-M	400	227.5
NiAT-M	399.1	226.2
NiIT	399.7	227.4
NiAT	398.9	226.5

SAED pattern of NiAT (Fig. S6)

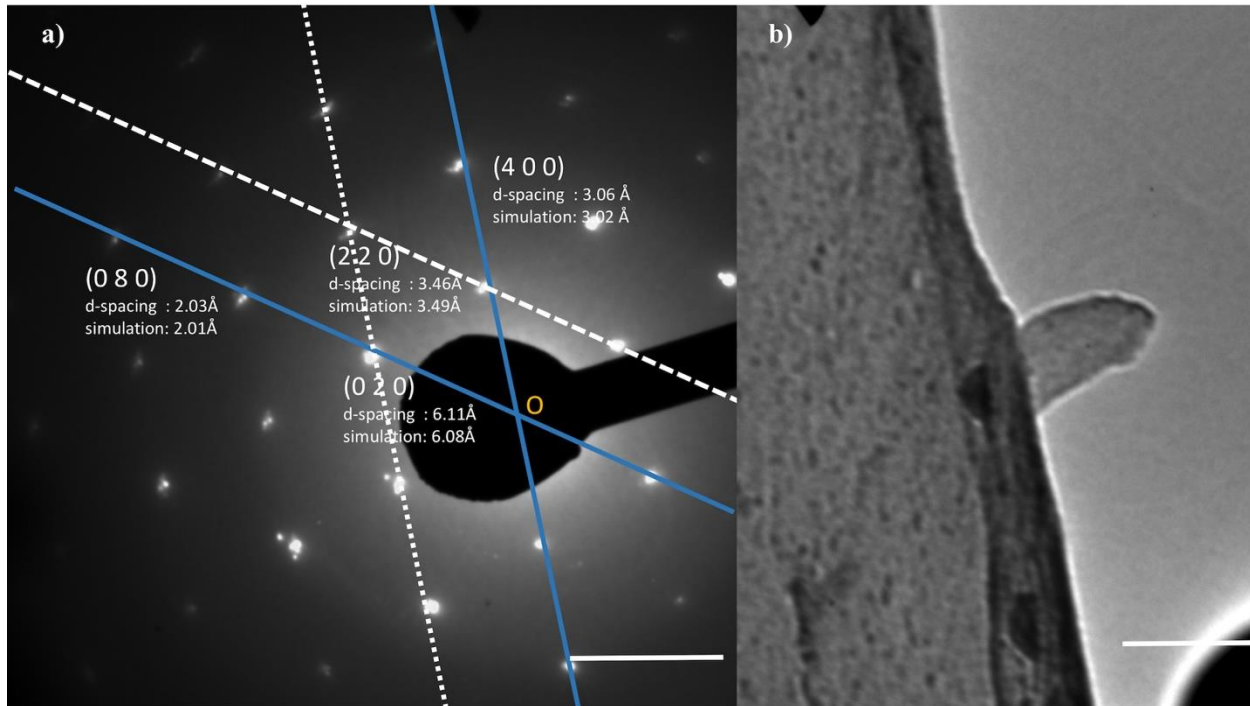


Fig. S6. **a)** SAED pattern of NiAT, scale bar  $2\text{nm}^{-1}$  **b)** TEM image which showed the SAED pattern, scale bar: 500 nm.

Simulation structure of NiAT (Fig. S7)

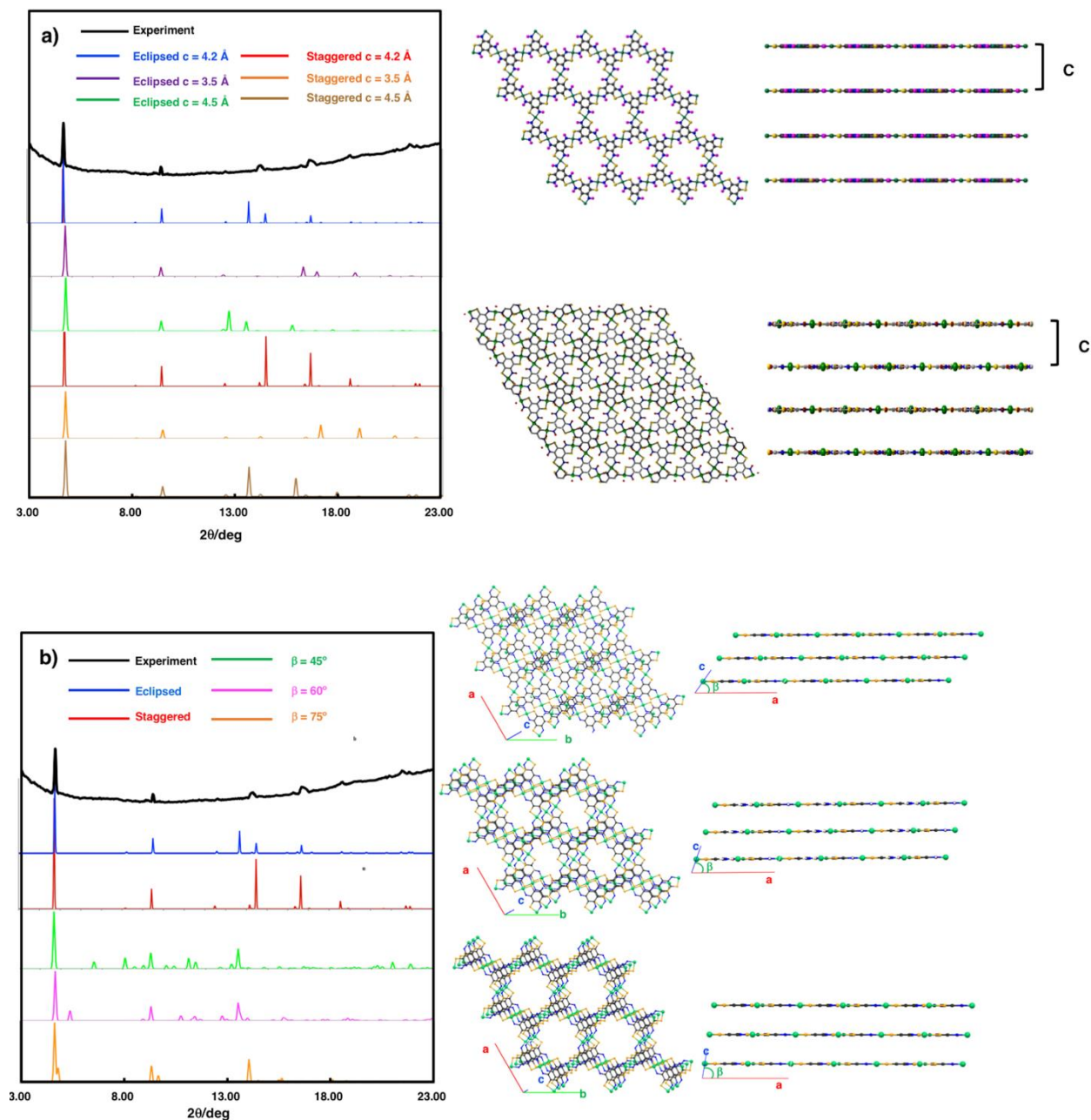


Fig. S7. **a)** The simulation structure using for eclipsed pattern. Space group:  $P3$ . Unit cell Length:  $a = b = 1.41 \text{ nm}$ . The interlayer distance,  $c$ , using  $0.42 \text{ nm}$ ,  $0.35 \text{ nm}$  and  $0.45 \text{ nm}$ . And the simulation structure using for staggered pattern. Space group:  $P-3$ , Unit cell Length:  $a = b = 1.405 \text{ nm}$ . The interlayer distance,  $c$ , using  $0.42 \text{ nm}$ ,  $0.35 \text{ nm}$  and  $0.45 \text{ nm}$ . **b)** The simulation structure using for eclipsed pattern. Space group:  $P3$ . Unit cell Length:  $a = b = 1.41 \text{ nm}$ . The interlayer distance is  $0.42 \text{ nm}$ . Modifying  $\beta$  angel to changing the stacking pattern.

Chemical conversion between **NiIT** and **NiAT** (Fig. S8)

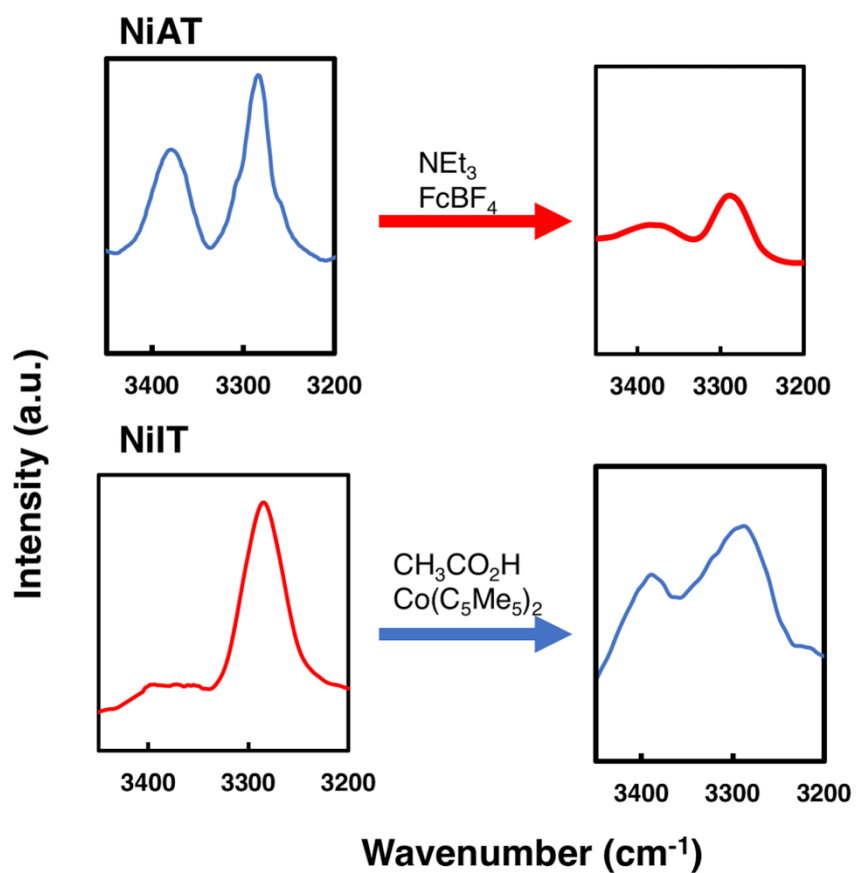


Fig. S8. **a** IR of **NiAT** before and after chemical oxidization. **b** IR of **NiIT** before and after chemical reduction.

Temperature dependent conductivity measurement of NiAT (Fig. S9)

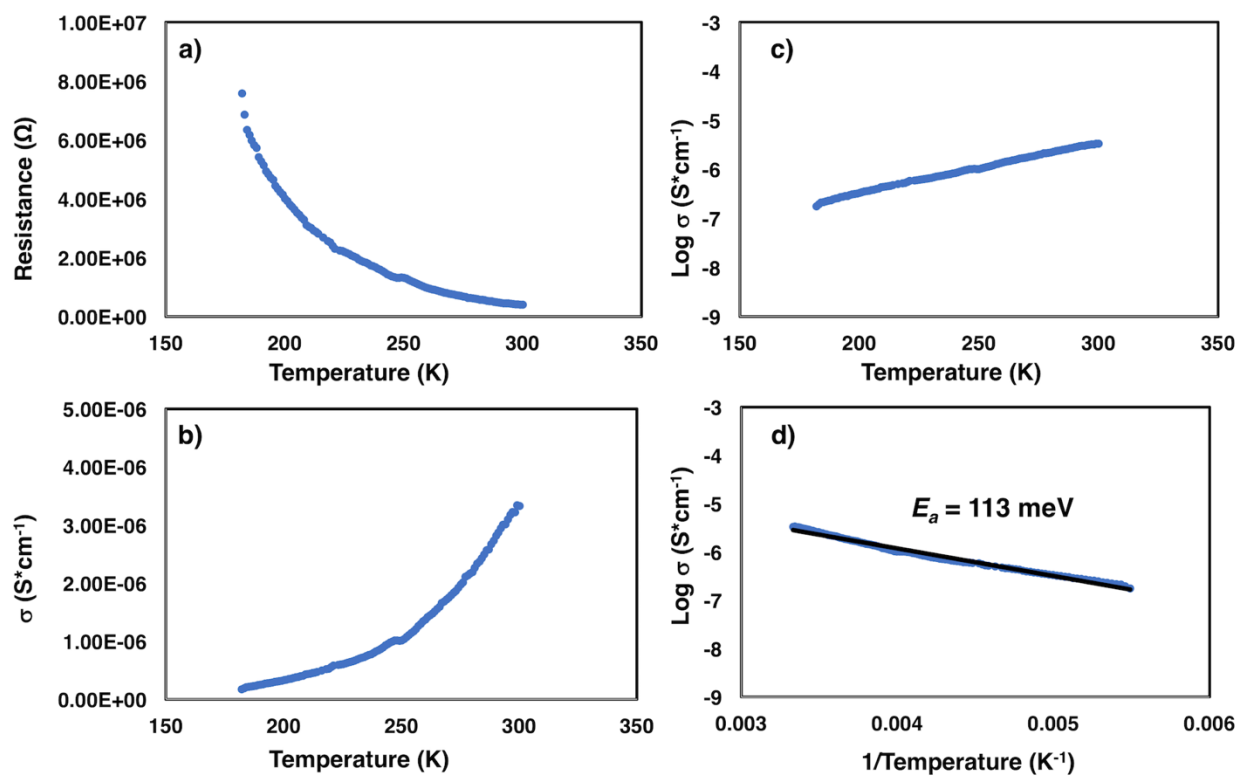


Fig. S9. **a**, Temperature depended resistance plot of NiAT. **b**, **c**, **d**, Temperature depended conductivity plot of NiAT.

Structures of **NiIT** and **NiAT** were used to calculate bands (Fig. S10)

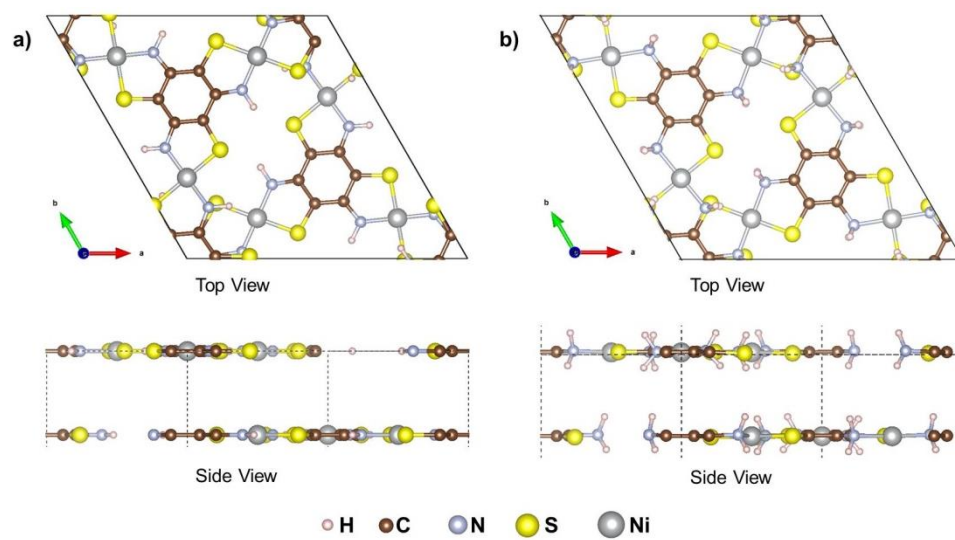


Fig. S10. Schematic representations of (a) **NiIT** and (b) **NiAT** structures to calculate bands.

MOs of NiIT and NiAT (Fig. S11)

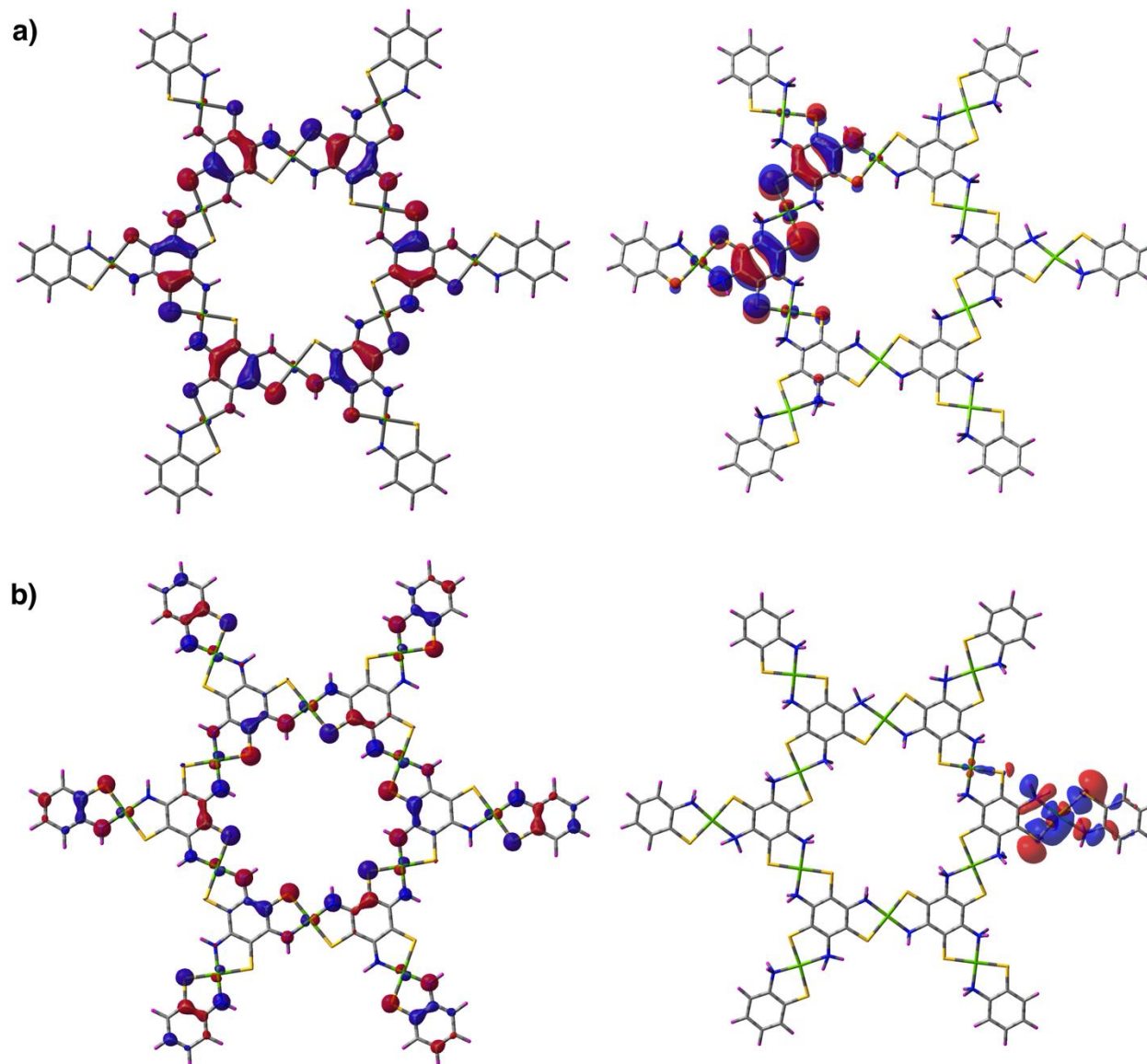


Fig. S11. **a)** Calculated MOs of NiIT (left) and NiAT (right) at HOMO level. **b)** Calculated MOs of NiIT (right) and NiAT (left) at LUMO level.

HER of NiAT at different pH value (Fig. S12)

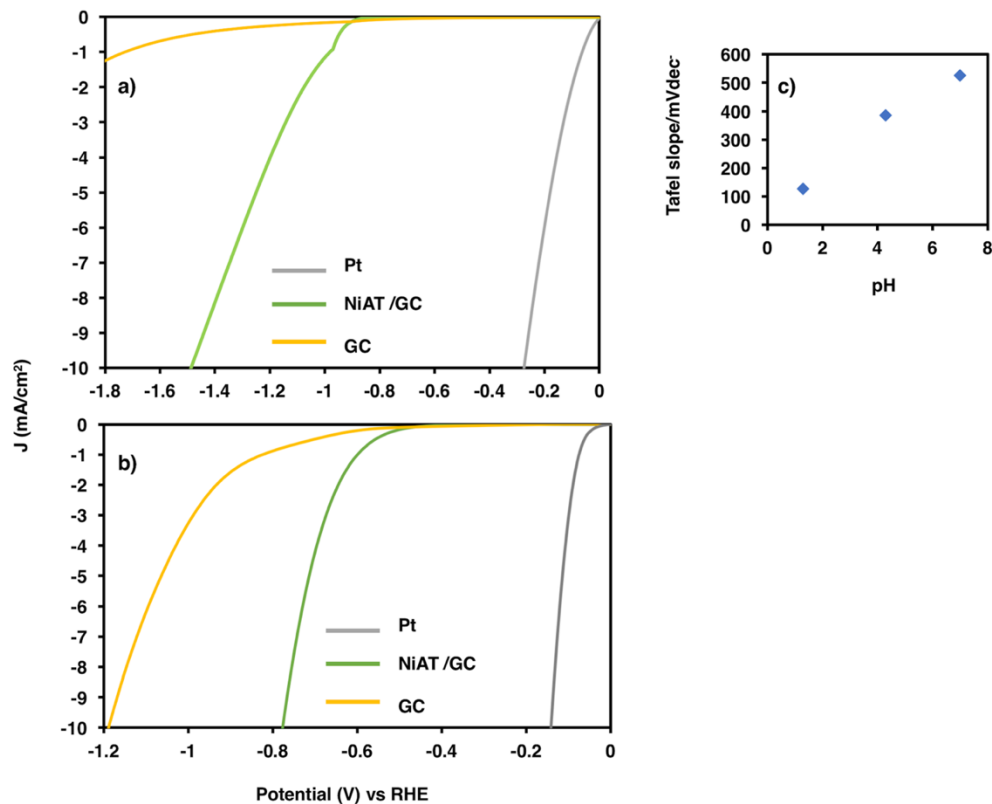


Fig. S12. **a)** Linear sweep voltammograms for HER reaction performed by Pt, NiAT/GC, GC under pH7 condition. **b)** Linear sweep voltammograms for HER reaction performed by Pt, NiAT/GC, GC under pH3.1 condition. **c)** And tafel plot.

Tafel slop and exchange current density ( $j_0$ ) of **NiAT** (Fig. S13)

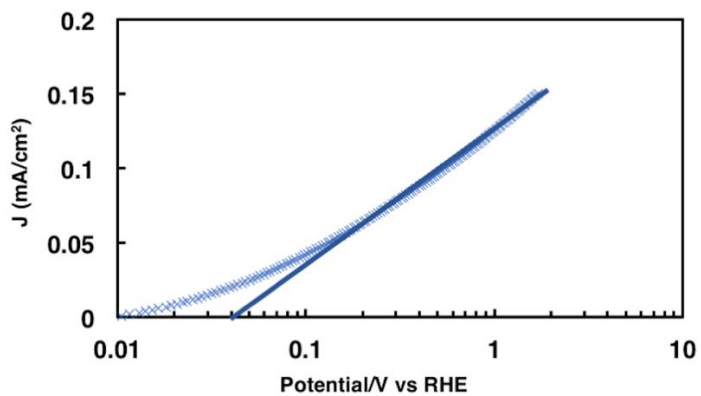


Fig. S13. Tafel slop and exchange current density ( $j_0$ ) of **NiAT**,  $j_0$  is estimated by linear fitting of the polarization curves using the Butler-Volmer equation.

Tafel slop and exchange current density ( $j_0$ ) of **NiAT** (Fig. S14)

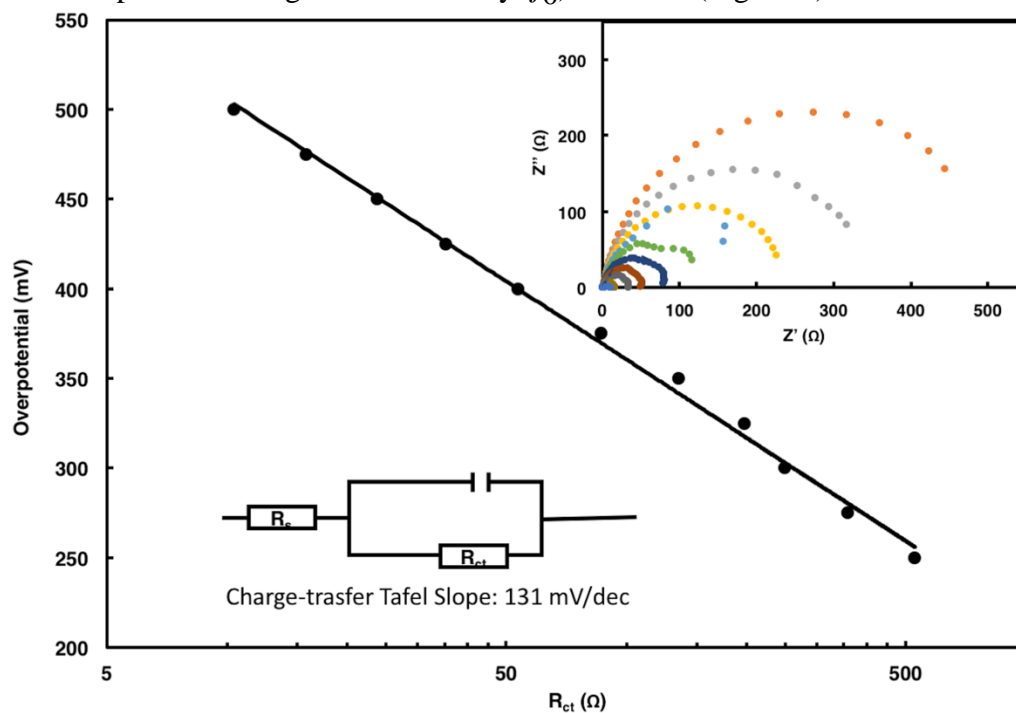


Fig. S14. Charge-transfer Tafel plots of **NiAT** from the Nyquist plots. Inset: Nyquist plots and fits of the impedance response of the vertically aligned **NiAT** sheet array catalyst under the overpotential from 250 mV to 500 mV in 25 mV increments, and the relating equivalent circuit that was used to fit the electrochemical impedance spectroscopy (EIS) data.  $R_s$  indicates the uncompensated series resistance, constant- phase element (CPE) refers to the double-layer capacitance under HER conditions, and  $R_{ct}$  represents the charge transfer resistance in the HER.

ECSA and TOF of NiAT (Figs. S15 and S16)

The density of the active sites on the surface can be identified by the electrochemical surface area (ECSA) of the NiAT. ECSA was calculated by testing the electrochemical double layer capacitance ( $C_{dl}$ ).

The specific capacitance can be calculated from the CV curve using the following equations:

$$C = \frac{\int ivdv}{2\mu m\Delta V} \quad (1)$$

where  $i$  and  $v$  are the current and potential in the CV test (A and V),  $\mu$  is the scan rate (V/s),  $m$  is the area of electrode ( $\text{cm}^2$ ),  $\Delta V$  is the potential window of discharge (0.1V here, Fig. S15). Resulted  $C_{dl}$  of 2.28 mF/ $\text{cm}^2$  and general specific capacitance of  $C_s = 0.12 \text{ mF}/\text{cm}^2$ .

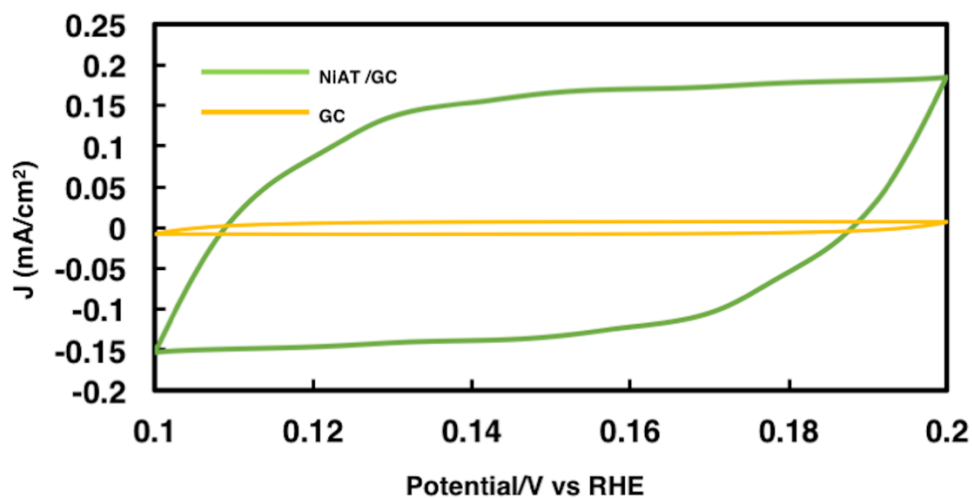


Fig. S15. Cyclic voltammograms (CV) curves of NiAT on glassy carbon electrode (NiAT/GC) and Nafion® dropped glassy carbon electrode (GC) in the region of 0.1~0.2 V vs. RHE at a scan rate of 50 mV s<sup>-1</sup>.

The ECSA of a catalyst can be calculated from the double layer capacitance ( $C_{dl}$ ) and  $C_s$  according equation (2):

$$ECSA = \frac{C_{dl}}{C_s} \quad (2)$$

TOF is calculated using the current density ( $j$ ) and the active site density ( $N$ ) according to the following equation:

$$TOF = \frac{\text{Total number of H}_2 \text{ molecules per second}}{\text{Total number of active sites per unit area}} = \frac{j}{2qN} \quad (3)$$

where  $q$  is the elementary charge as  $1.6 \times 10^{-19}$ , and 2 accounts for 2 electrons transfer per one  $H_2$  molecule generation. The density of HER active sites in Ni atoms in **NiAT** is  $7.21 \times 10^{18}$  Ni atoms per  $cm^2$  according to equation (4):

$$\#_{Ni}(0.2mg) = \frac{(0.2 / 0.07) \frac{mg}{cm^2}}{608.73 \frac{g}{mol}} 6.022 \times 10^{23} \times 3 = 7.21 \times 10^{18} \quad (4)$$

So the active TOF of Ni is calculated according to equation (5):

$$TOF_{Ni} = \frac{j}{2 \times 1.6 \times 10^{-19} \times \#_{Ni}(0.2mg) \times ECSA} \quad (5)$$

The calculated TOF (Fig. S16) of **NiAT**.

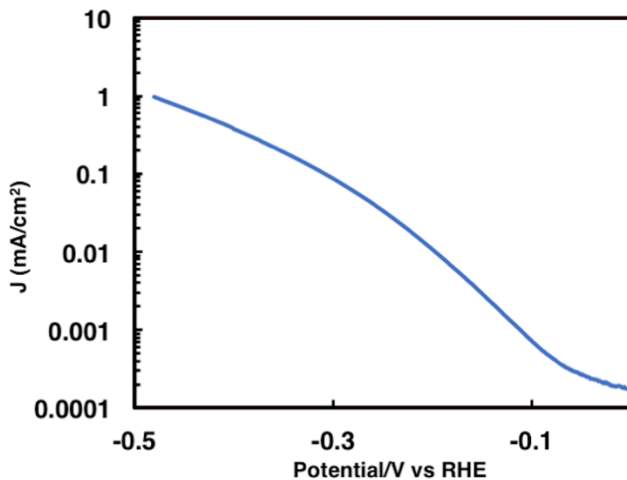


Fig. S16. Plot that displays the turnover frequency (TOF) per Ni atom **NiAT** catalyts.

Durability of NiAT for 500 cycles of HER (Figs. S17 and S18)

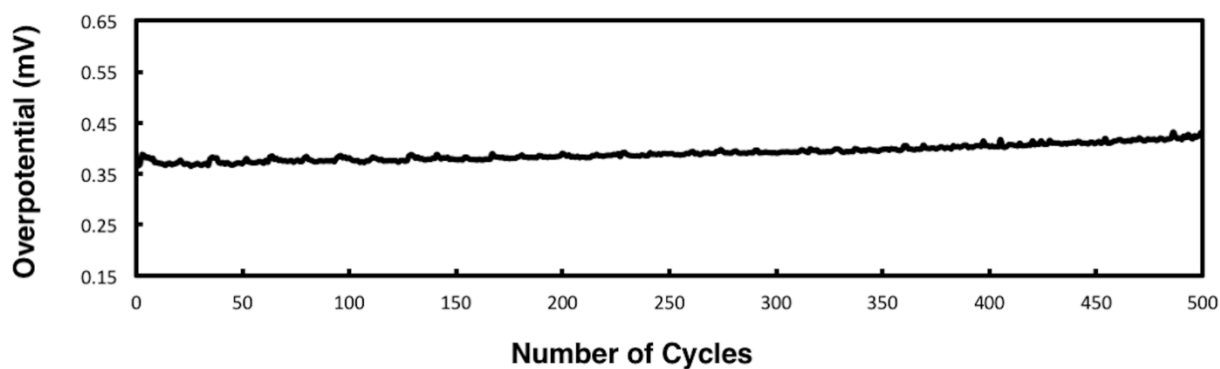


Fig. S17. Operating potential versus HER Cycles at  $10 \text{ mA cm}^{-2}$ .

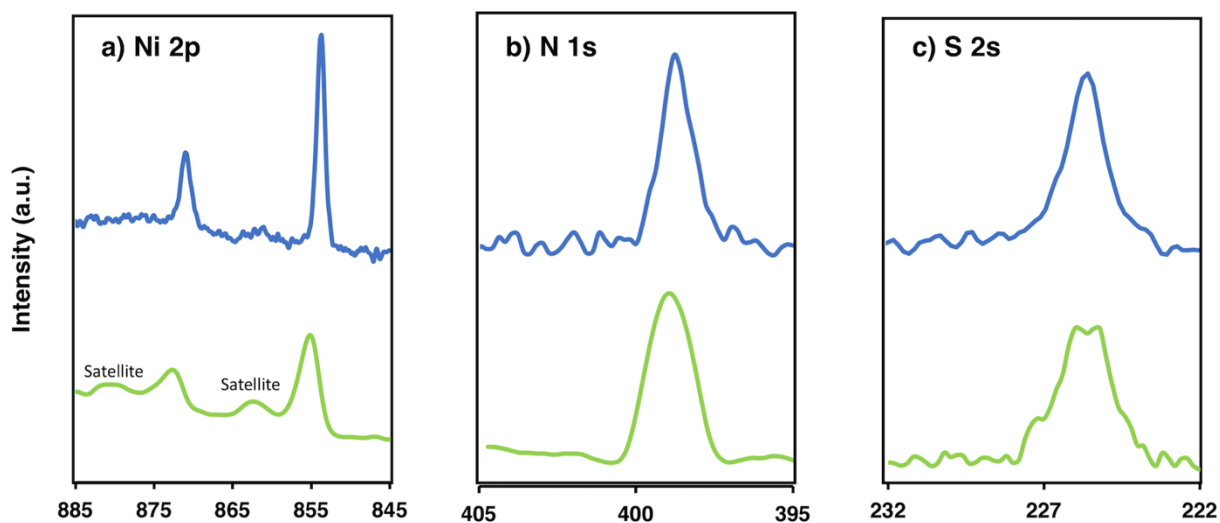


Fig. S18. **a)** Narrow-scan X-ray photoelectron spectroscopy (XPS) focusing on the N 1s region. **b)** Focusing on the S 2s region. **c)** Focusing on the Ni 2p region. Upper (red curve) before HER, lower (green curve) after HER.